Journal of Solid State Chemistry 184 (2011) 3228–3231

Contents lists available at SciVerse ScienceDirect

Journal of Solid State Chemistry

journal homepage: www.elsevier.com/locate/jssc

Unusual oxidation states give reversible room temperature magnetocaloric effect on perovskite-related oxides $SrFe_{0.5}Co_{0.5}O_3$

C. Yin, Q. Liu, R. Decourt, M. Pollet, E. Gaudin, O. Toulemonde *

CNRS, Université de Bordeaux, ICMCB, 87 avenue du Dr. A. Schweitzer, Pessac F-33608, France

ARTICLE INFO

Article history:
Received 3 June 2011
Received in revised form
26 September 2011
Accepted 3 October 2011
Available online 8 October 2011

Keywords:
Electrochemical oxidation
Ferromagnetism
$SrFe_{0.5}Co_{0.5}O_3$
Magnetocaloric effect

ABSTRACT

The magnetic properties and the magnetocaloric effect are presented for the perovskite-related oxide $SrFe_{0.5}Co_{0.5}O_3$ prepared using electrochemical oxidation. $SrFe_{0.5}Co_{0.5}O_3$ exhibits a second order paramagnetic–ferromagnetic transition close to room temperature (T_C=330 K). The maximal magnetic entropy change ΔS_M^{Max}, the maximal adiabatic temperature change ΔT_{ad} and the refrigerant capacity are found to be equal to respectively 4.0 J/kgK, 1.8 K and 258 J/kg while raising the B-field change from 0 to 5 T.

Nowadays searching for energy saving products is an important issue regarding the sustainable approach. Towards a higher energetically efficiency, a promising alternative technology is the magnetic refrigeration based on the magnetocaloric effect (MCE). Furthermore, it is believed to be more eco-friendly than the conventional gas compression refrigeration.

The MCE reaches its maximum value at the paramagnetic (PM) to ferromagnetic (FM) transition temperature (T_C) where the magnetic entropy change is maximum. As a consequence, materials exhibiting large saturation magnetization are particularly appealing and numerous intermetallic compounds were reported like *e.g.* $Gd_5(Si,Ge)_4$[1], $MnAs_{1-x}Sb_x$ [2,3] and $La(Fe,Si)_{13}$ [4,5] materials (see also references therein and the special issue on magnetocaloric materials [6]). Such materials however generally suffer from their relative high cost, their toxicity and/or their poor resistance to oxidation process. This later point is especially in favor of the recent studies made on oxide materials though extensive ageing studies are still required to confirm this assertion. One can also notice that there is a need for further improved materials considering that none of the known materials have yet been employed in a commercial refrigerator.

In this communication, we focus on the oxide based materials. Till now most of the works dealing with oxide materials report on mixed valence manganites with general formula $R_{1-x}A_xMnO_3$ (R=La, Nd, etc., and A=Ca, Sr, etc.) neglecting alternative transition metal oxide families [7,8]. We propose an alternative approach focused on perovskite related oxide $SrFe_{0.5}Co_{0.5}O_3$. It is a well known FM whose properties are due to an unusually high oxidation state [9,10]. We report here for the first time on its relatively appealing MC properties.

Polycrystalline $SrFe_{0.5}Co_{0.5}O_3$ sample was synthesized in two steps. First, an oxygen deficient $SrFe_{0.5}Co_{0.5}O_{3-\delta}$ pellet was obtained by conventional solid state reaction [11]. Then, electrochemical oxidation was employed to fill the oxygen vacancies [12]. Powder X-ray diffraction (XRD) was performed on a PANalytical X'Pert Pro diffractometer with monochromatized Cu$K\alpha_1$ radiation (Fig. 1). The general structure analysis system (GSAS) package was used to fit the X-ray diffraction profiles [13]. As shown in Fig. 1, the full pattern matching analysis of the XRD data shows that the electrochemically oxidized phase crystallizes in a single cubic perovskite structure with space group $Pm\bar{3}m$ and refined lattice parameter a=3.8335(1) Å at room temperature. If a deviation from the simple cubic to tetragonal ($I4/mmm$) perovskite structure would occur reflecting a significant oxygen deficiency, an extra peak would be seen at low angle [14]. The inset highlights that none of the superstructure peaks of this tetragonal phase is seen in the diffractograms within the X-ray detection limit. However, observation of cubic perovskite symmetry does not insure a high oxidation state as recently highlighted for $SrFe_{0.5}Co_{0.5}O_{2.88}$ [10]. An easy way to check it is to measure the magnetic properties. Indeed there is a direct correlation between the value of the Curie temperature T_C and the oxidation state. It was previously observed that T_c is equal to approximately 250 K ± 10 K for $SrFe_{0.5}Co_{0.5}O_{2.88}$ [10] (considering the minimum value of the slope of the magnetization curve $M=f(T)$) and to 340 K for $SrFe_{0.5}Co_{0.5}O_{3-\delta}$(with $\delta < 0.06$) [15]. For our sample the

* Corresponding author.
E-mail address: toulemon@icmcb-bordeaux.cnrs.fr (O. Toulemonde).

0022-4596/$ - see front matter © 2011 Elsevier Inc. All rights reserved.
doi:10.1016/j.jssc.2011.10.002

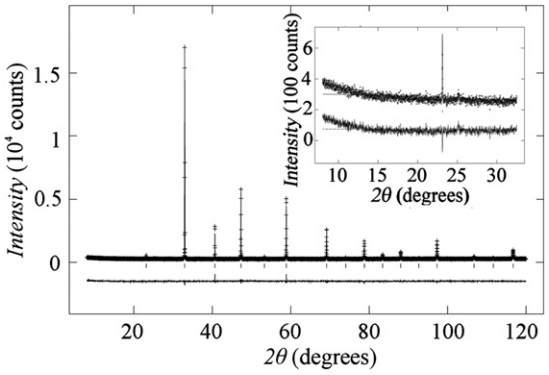

Fig. 1. Observed, calculated and difference X-ray diffraction profile plots for $SrFe_{0.5}Co_{0.5}O_3$.

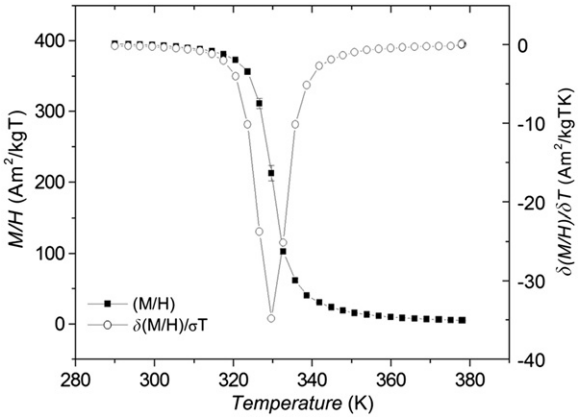

Fig. 2. Magnetization for $SrFe_{0.5}Co_{0.5}O_3$ sample with temperature increasing from 290 K to 375 K under constant magnetic field 100 G.

T_c value estimated from the derivative curve dM/dT is equal to 330 K ± 5 K and confirms its high oxidation state (Fig. 2). As previously observed after electrochemical oxidation process [15], a possible oxygen release can be then followed through magnetization measurement. Consequently, the sample was capped to prevent any loss of oxygen during the magnetic measurement. Resistivity measurement was also carried out using a home-made four-probe dc conductivity measurement setup (Fig. 3). A typical metal-like conductor is observed for the first time, which is similar to that of $SrFeO_3$ and $SrCoO_3$ phases [16,17]. All these results converge to the same conclusion that our $SrFe_{0.5}Co_{0.5}O_{3-\delta}$ sample has a high oxygen content and the low value of the oxygen deficiency δ will not be further considered in the present manuscript.

Fig. 4 shows some selected M–B plots at 5 K and for a series of temperature between 285 K and 375 K when applied magnetic field goes up to 5 T; all the presented acquisitions were made on increasing the magnetic field. They are characteristic of a soft ferromagnet with a rapid increase in the magnetization at low field (≤ 0.1 T) and a slow asymptotic regime at high field. A very small magnetic hysteresis is also observed with a remanent magnetization M_R around 1 Am^2/kg suggesting that the PM to FM transition is of second order. A data treatment within the mean field theory following the $H/M=f(M^2)$ Arrott-plot approach exhibits a positive slope near the Curie temperature (Fig. 5). It further supports the second order character of the magnetic transition according to Banerjee's criteria [18]. The saturation magnetization M_S obtained from the 5 K M–B curve is 3 μ_B per formula unit as previously reported [9]. From this value and the previously reported high spin ground state for Fe^{4+} ($t_{2g}^3e_g^1$

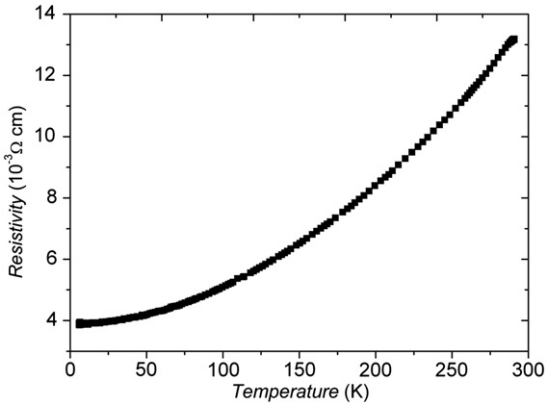

Fig. 3. Temperature dependent resistivity indicating a metallic behavior for $SrFe_{0.5}Co_{0.5}O_3$ sample.

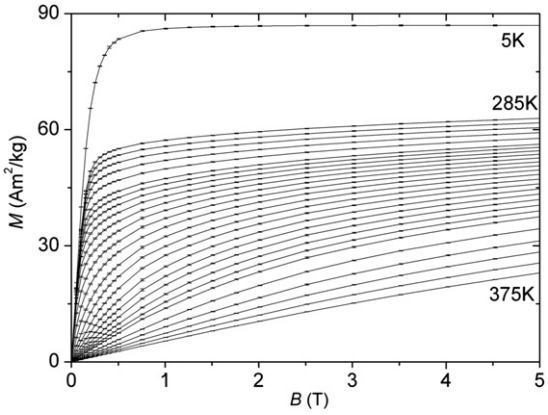

Fig. 4. Magnetization isotherms of $SrFe_{0.5}Co_{0.5}O_3$ measured on increasing field up to 5 T. The temperature interval is 2.5 K between 310 K and 350 K and 5 K out of this range.

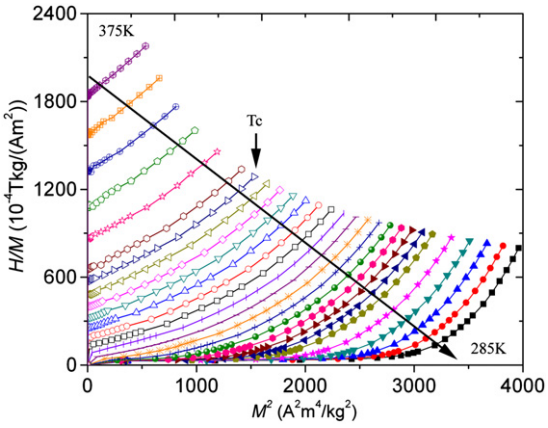

Fig. 5. Arrott plots of $SrFe_{0.5}Co_{0.5}O_3$.

$\mu_S=4\ \mu_B$) [12], one can speculate an average spin value $\mu_S=2\ \mu_B$ per Co^{4+} per formula unit. Based on a spin-only ionic model and excluding any oxygen deficiency, the Co^{4+} ground state may probably be described by a mixture of 75% LS state ($t_{2g}^5e_g^0$) and 25% HS state ($t_{2g}^3e_g^2$). The real ground states may however be more complex if one takes into account a possible slight oxygen non-stoichiometry, the $3d^5\underline{L}$ and $3d^6\underline{L}$ character for respectively Fe^{4+} and Co^{4+} ground states ($\underline{L}$ denotes a ligand hole on the oxygen 2p band) as supported by the X-ray absorption spectrum (XAS) [19] and/or the itinerant character of the electrons as previously reported in $SrCoO_3$ [17]. Consequently, far away from the aim of

this manuscript, the determination of the ground states for Co^{4+} and Fe^{4+} that is a critical feature for these oxides showing coexistence of itinerant and localized electrons, is a study itself requiring for instance X-ray absorption spectroscopy supported by a theoretical approach [20] and Seebeck coefficient measurement on the same phase [21,22].

Thermodynamically, the MCE is obtained by calculating the magnetic entropy change ΔS_M. From the magnetization data shown in Fig. 4, we apply the Maxwell relation

$$\Delta S_M = \frac{1}{\Delta T}\left[\int_0^{B'} M(T+\Delta T,B)dB - \int_0^{B'} M(T,B)dB\right]$$

where $M(T,B)$ and $M(T+\Delta T,B)$ represent the values of the magnetization in a magnetic B-field at the temperature T and $T+\Delta T$, respectively.

The $-\Delta S_M$ maxima of $SrFe_{0.5}Co_{0.5}O_3$ occurring at the Curie temperature are slightly shifted toward high temperature when magnetic B-field increases (Fig. 6). They vary from 1.3 to 4.0 J/kg K and represent about 58%–47% of that of Gd [23]. Moreover, $-\Delta S_M$ remains uniform over a broad range of temperature as expected for a second-order magnetic transition (SOMT) materials. But it could also be due to a chemical heterogeneity effect related to the random distribution of Fe^{4+} and Co^{4+} on the perovskite B-site. This broad range of temperature is desirable for an Ericson-cycle magnetic refrigerator. Next, the so-called relative cooling power (RCP) related to refrigerant capacity was also calculated as the product of ΔS_M maximum and the full width at half maximum δT_{FWHM} ($RCP = \Delta S_M^{max} \times \delta T_{FWHM}$). The RCP versus B of $SrFe_{0.5}Co_{0.5}O_3$ is plotted in Fig. 6 inset. A linear behavior is emphasized. For $\Delta B = 1$–5 T, it reaches from 38 to 258 J/kg, which is about 56%−50% of that of Gd. Finally, to gain a better insight on the opportunity to use the $SrFe_{0.5}Co_{0.5}O_3$ compound for the magnetic cooling process, the determination of the adiabatic temperature difference ΔT_{ad} is required. The total entropy $S(0,T)$ under zero B-field can be calculated from the heat capacity data as

$$S(0,T) = \int_0^T \frac{C(0,T)}{T} dT$$

The $S(B,T)$ is then determined by subtracting the corresponding ΔS_M from S(0,T). It allows to obtain the adiabatic temperature difference ΔT_{ad} from the isentropic difference between the entropy curves $S(0,T)$ and $S(B,T)$ (Fig. 7). The maximum of the peak of the each curve corresponds to $\Delta T_{ad} = 0.5$, 0.9, 1.2, 1.5 and 1.8 K for a B-field change from 0 to 1, 2, 3, 4 and 5 T, respectively. It should be pointed out that ΔT_{ad} is higher than 1 K within a large range of temperature from 300 K to 375 K when $\Delta B = 5$ T. This highlights that $SrFe_{0.5}Co_{0.5}O_3$ could be used for the magnetic cooling in a large temperature range including RT despite its high ordering temperature (but unfortunately for a large applied magnetic field). Analysis of the heat capacity data (Fig. 7) shows that it increases smoothly with the temperature and does not exhibit any clear indication of a well-defined ordering transition. Indeed, the expected punctual anomaly at T_C is distributed over a broad peak at the FM–PM transition likely correlated with the chemical heterogeneity effect that spreads out the magnetic interactions.

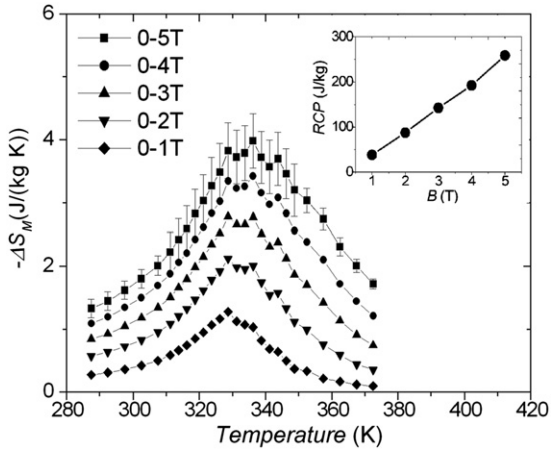

Fig. 6. Temperature dependent magnetic entropy change of $SrFe_{0.5}Co_{0.5}O_3$ for a B-field variation from 0–1 to 0–5 T. Error bars are included for $\Delta B = 5$ T, inset shows the B-field dependent of RCP.

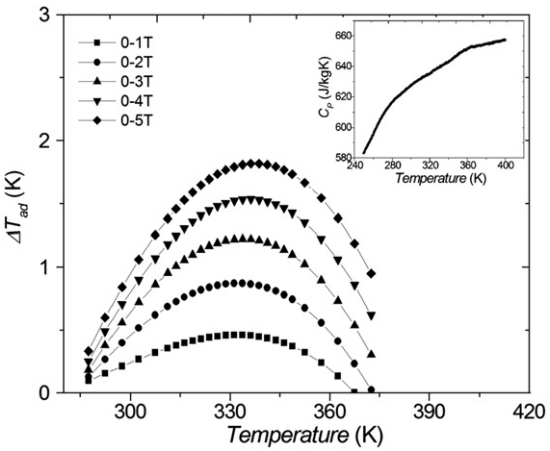

Fig. 7. Temperature dependent adiabatic temperature change of $SrFe_{0.5}Co_{0.5}O_3$ for a B-field variation from 0–1 to 0–5 T. Inset shows temperature dependent heat capacity C_P under zero B-field.

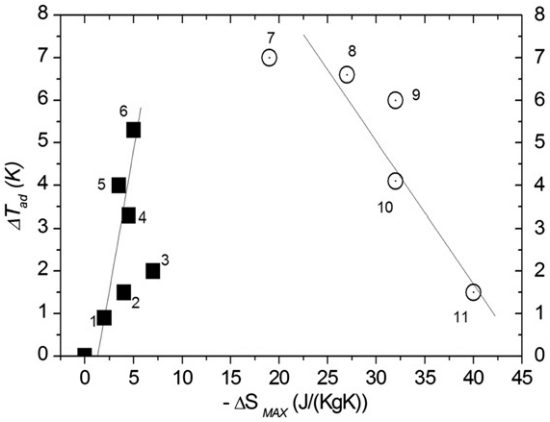

Fig. 8. The adiabatic temperature change ΔT_{ad} versus the isothermal entropy change $|\Delta S_M|$ for $\Delta B = 0$–2 T change for: 1. $SrFe_{0.5}Co_{0.5}O_3$ (present work) 2. $CdCr_2S_4$ ($T_C = 87$ K) [24] 3. $LaFe_{11}Co_{0.9}Si_{1.1}$ ($T_C = 295$ K) [25] 4. $La_{0.7}Ca_{0.2}Sr_{0.1}MnO_3$ ($T_C = 297$ K) [26] 5. $Gd_{71}Fe_3Al_{26}$ ($T_C = 118$ K) [27] 6. Gd ($T_C = 294$ K) [23] 7. $La(Fe_{11.4},Si_{1.6})H_{1.5}$ ($T_C = 325$ K) [5] 8. $Gd_5Si_2Ge_2$ ($T_C = 270$ K) [1] 9. $MnFeP_{0.5}As_{0.3}Si_{0.2}$ ($T_C = 296$ K) [28] 10. MnAs ($T_C = 315$ K) [2] 11. $Ni_{55}Mn_{20}Ga_{25}$ ($T_C = 315$ K) [29]. Lines are guide for eyes. Empty ring and full squared symbols indicate FOMT and SOMT materials, respectively.

Finally, for comparison, we summarize both $|\Delta S_M|$ and ΔT_{ad} for $\Delta B = 2$ T of some promising MCE candidates Fig. 8. Most of them are suitable at room temperature. Given that the magnetic entropy change is often overestimated for first-order magnetic transition (FOMT) materials [30,31], Fig. 8 highlights that the ΔT_{ad} value is a significant parameter to quantify the MCE. The candidates are divided into two groups depending on the order parameter describing the magnetic phase transition.

$Gd_5Si_2Ge_2$, $Ni_{55}Mn_{20}Ga_{25}$, MnAs, $MnFeP_{0.5}As_{0.3}Si_{0.2}$ and $La(Fe_{11.4},Si_{1.6})H_{1.5}$ experience FOMT and show both large MCE

and the highest ΔT_{ad} value (right panel on Fig. 8) what would make them the most promising candidates for MCE applications. Several points however can be cited that cloud this picture: (i) a thermal hysteresis is commonly present in FOMT materials, making them less suitable for applications focused on a targeted range of temperature; (ii) the FOMT is necessarily coupled to another transition (*e.g.* structural distortion, sharp change in the volume) that can hinder the cyclability of the material especially when working at high frequency; (iii) the adiabatic magnetization step decreases the magnetic entropy and induces the warming of the sample what, in turn, can stabilize the high temperature nuclear phase with a higher configuration entropy what is likely to decrease the global efficiency of the step; such competition between the two phenomena needs to be studied.

The others phases show second-order magnetic transition (SOMT) and have relatively smaller MCE (left panel on Fig. 8). This disadvantage can be compensated by high working frequencies in real operation due to the absence of thermal hysteresis. More interesting is that the $|\Delta S_M| - \Delta T_{ad}$ plot sheds in light that the ΔT_{ad} of the SOMT materials increases continuously with $|\Delta S_M|$ contrary to the FOMT materials. Even if the shown data are restricted to the disorder–order magnetic transition, such tendency suggests that our approach on SOMT transition is complementary to the one focused on the magnetostructural transition. In addition, as already pointed out, it is likely that the oxides would be less impacted by ageing effects than the Gd and/or intermetallic materials [32]. Furthermore, $SrFe_{0.5}Co_{0.5}O_3$ has a metallic conductivity; in accordance with the Wiedemann–Franz law [33], it may result in a high thermal conductivity appropriate for practical applications to insure good heat exchange. Finally, as shown in Fig. 8, the titled oxide $SrFe_{0.5}Co_{0.5}O_3$ as well as some manganites have a lower $|\Delta S_M|$ value than Gd material however it is also much cheaper. Regarding all these results and remarks, the system Sr–Fe–Co–O deserves to be deeper studied as potential candidate for near room temperature refrigeration.

In conclusion, we synthesized the unusually high stoichiometric $SrFe_{0.5}Co_{0.5}O_{3-\delta}$ oxide using electrochemical oxidation. The sample has a metallic conductivity within the probed temperature range [5K–290 K] and a second order PM–FM transition around 330 K is evidenced from the temperature dependence of the magnetization curves. The magnetocaloric properties were extracted from the magnetization and heat capacity measurement. The magnetic entropy change ΔS_M (4.0 J/(kg K)), the moderate adiabatic temperature change ΔT_{ad} (1.8 K) associated with a high RCP value (258 J/kg) observed for $\Delta B = 5$ T around T_C are as large as the ones reported for manganites what sheds light on our new approach on oxide materials. Our work may especially opens a new material system Sr–Fe–Co–O perovskites for further studies on SOMT materials to improve the MCE.

This work has been supported by the European project "SOPRANO" under Marie Curie actions (Grant no. PITNGA-2008–214040) and the French CNRS project "Programme Interdisciplinaire ENERGIE".

References

[1] V.K. Pecharsky, K.A. Gschneidner Jr., Appl. Phys. Lett. 70 (1997) 3299.
[2] H. Wada, Y. Tanabe, Appl. Phys. Lett. 79 (2001) 3302.
[3] O. Tegus, E. Bruck, K.H.J. Buschow, F.R. de Boer, Nature 415 (2002) 150.
[4] F.X. Hu, B.G. Shen, J.R. Sun, Z.H. Cheng, G.H. Rao, X.X. Zhang, Appl. Phys. Lett. 78 (2001) 3675.
[5] A. Fujita, S. Fujieda, Y. Hasegawa, K. Fukamichi, Phys. Rev. B 67 (2003) 104416.
[6] E. Bruck, co-authors, J. Magn. Magn. Mater 321 (2009) 21 special issue.
[7] M.H. Phan, S.C. Yu, J. Magn. Magn. Mater. 308 (2007) 325.
[8] Y. Sun, M.B. Salamon, S.H. Chun, J. Appl. Phys. 92 (2002) 3235.
[9] S. Kawasaki, M. Takano, Y. Takeda, J. Solid State Chem. 121 (1996) 174.
[10] A. Munoz, J.A. Alonso, M.J. Martinez-Lope, C. de la Calle, M.T. Fernandez-Diaz, J. Solid State Chem. 179 (2006) 3365.
[11] A. Maignan, C. Martin, N. Nguyen, B. Raveau, Solid State Sci. 3 (2001) 57.
[12] P. Bezdicka, L. Fournès, A. Wattiaux, J.C. Grenier, M. Pouchard., Solid State Comm 91 (1994) 501.
[13] A.C. Larson and R.B. Von Dreele, Los Alamos National Laboratory Report No. LAUR 86–748, 2004 (unpublished).
[14] K. Świerczek, B. Dabrowski, L. Suescun, S. Kolesnik, J. Solid State Chem. 182 (2009) 280.
[15] C. Okazoe, Y. Takeda, N. Imanishi, O. Yamamoto, M. Takano, R. Kanno, Solid State Ionics 86–88 (1996) 1431.
[16] P. Adler, A. Lebon, V. Damljanovic, C. Ulrich, C. Bernhard, A.V. Boris, A. Maljuk, C.T. Lin, B. Keimer, Phys. Rev. B 73 (2006) 094451.
[17] P. Bezdicka, A. Wattiaux, J.C. Grenier, M. Pouchard, P. Hagenmuller, Z. Anorg. Allg. Chem 619 (1993) 7.
[18] S.K. Banerjee, Phys. Lett 12 (1964) 16.
[19] M. Abbate, G. Zampieri, J. Okamoto, A. Fujimori, S. Kawasaki, M. Takano, Phys. Rev. B 65 (2002) 165120.
[20] M. Pouchard, A. Villessuzane, J.P. Doumerc, J. Solid State Chem 162 (2001) 282.
[21] W. Koshibae, K. Tsutsui, S. Maekawa, Phys. Rev. B 62 (2000) 6869.
[22] M. Pollet, J.P. Doumerc, E. Guilmeau, D. Grebille, J.F. Fagnard, R. Cloots, J. Appl. Phys 101 (2007) 083708.
[23] S. Yu. Dan'kov, A.M. Tishin, V.K. Pecharsky, and K.A. Gschneidner, Jr., Phys. Rev. B 57 (1998) 3478 and O. Tegus (Seminar WZI Amsterdam, 2003).
[24] L.Q. Yan, J. Shen, Y.X. Li, F.W. Wang, Z.W. Jiang, F.X. Hu, J.R. Sun, B.G. Shen, Appl. Phys. Lett. 90 (2007) 262502.
[25] M. Balli, D. Fruchart, O. Sari, D. Gignoux, J.H. Huang, J. Hu, P.W. Egolf, J. Appl. Phys 106 (2009) 023902.
[26] A.N. Ulyanov, J.S. Kim, Y.M. Kang, D.G. Yoo, S.I. Yoo, J. Appl. Phys. 104 (2008) 113916.
[27] Q.Y. Dong, B.G. Shen, J. Chen, J. Shen, F. Wang, H.W. Zhang, J.R. Sun, J. Appl. Phys. 105 (2009) 053908.
[28] W. Dagula, O. Tegus, X.W. Li, L. Song, E. Bruck, D.T. Cam Thanh, F.R. de Boer, K.H.J. Buschow, J. Appl. Phys 99 (2006) 08Q105.
[29] M. Pasquale, C.P. Sasso, L.H. Lewis, L. Giudici, T. Lograsso, D. Schlagel, Phys. Rev. B 72 (2005) 094435.
[30] J.S. Amaral, V.S. Amaral Appl., Phys. Lett 94 (2009) 042506.
[31] W.B. Cui, W. Liu, Z. Zhang, Appl. Phys. Lett. 96 (2010) 222509.
[32] F. Canepa, S. Cirafici, M. Napoletano, M.R. Cimberle, L. Tagliafico, F. Scarpa, J. Phys. D: Appl. Phys 41 (2008) 155004.
[33] C. Kittel, Introduction to Solid State Physics, seventh ed., Wiley, New York, 1996.